nature medicine

Somatostatin regulates brain amyloid β peptide $A\beta_{42}$ through modulation of proteolytic degradation

Takashi Saito[1,2], Nobuhisa Iwata[1,2], Satoshi Tsubuki[1], Yoshie Takaki[1], Jiro Takano[1], Shu-Ming Huang[1], Takahiro Suemoto[1], Makoto Higuchi[1] & Takaomi C Saido[1]

Expression of somatostatin in the brain declines during aging in various mammals including apes and humans[1,2]. A prominent decrease in this neuropeptide also represents a pathological characteristic of Alzheimer disease[3,4]. Using *in vitro* and *in vivo* paradigms, we show that somatostatin regulates the metabolism of amyloid β peptide (Aβ), the primary pathogenic agent of Alzheimer disease, in the brain through modulating proteolytic degradation catalyzed by neprilysin. Among various effector candidates, only somatostatin upregulated neprilysin activity in primary cortical neurons. A genetic deficiency of somatostatin altered hippocampal neprilysin activity and localization, and increased the quantity of a hydrophobic 42-mer form of Aβ, $A\beta_{42}$, in a manner similar to presenilin gene mutations that cause familial Alzheimer disease. These results indicate that the aging-induced downregulation of somatostatin expression may be a trigger for Aβ accumulation leading to late-onset sporadic Alzheimer disease, and suggest that somatostatin receptors may be pharmacological-target candidates for prevention and treatment of Alzheimer disease.

An abnormally high level of Aβ in brain seems to have a central role in the pathogenesis of Alzheimer disease[5]. In particular, analyses of several familial Alzheimer disease–causing mutations in genes encoding amyloid precursor protein (APP) and presenilin have established the importance of generation of $A\beta_{42}$, a 42-mer form of the peptide that has a higher amyloidogenic potency than $A\beta_{40}$. Based on the hypothesis that Aβ amyloidosis in sporadic (nonfamilial) Alzheimer disease, which comprises more than 90% of all cases of Alzheimer disease, may be caused by the deceleration of Aβ degradation, we previously identified neprilysin as a physiological Aβ-degrading peptidase and showed that neprilysin regulates the steady-state levels of both $A\beta_{40}$ and $A\beta_{42}$ *in vivo*[6,7]. Neprilysin expression in the brain decreases during aging and in the early stages of Alzheimer disease progression[8,9], whereas elevated neprilysin activity has been shown to reduce the accumulation of both soluble and fibrillar Aβ in APP transgenic mice[10,11]. Identification of a pharmacological means to selectively upregulate brain neprilysin activity would therefore provide a new therapeutic opportunity. A rationale for this strategy is based on the fact that at least two cell type–specific ligands capable of upregulating neprilysin activity have been identified: opioid for monocytes[12] and substance P for bone marrow cells[13].

In our search for such a potential 'activator' of brain neprilysin, we first performed a series of unbiased screens for a ligand that alters neprilysin activity in primary cortical neurons using an activity staining method. This method visualizes enzymatically active neprilysin on the cell surface and was used because endogenous neprilysin in primary neurons is difficult to detect by immunocytochemistry[14], enzymatically active neprilysin requires a post-translational maturation (such as glycosylation) for its full activity[14] and cell-surface neprilysin has a more important role in degrading the primary pathogenic form of Aβ, $A\beta_{42}$, than the intracellular activity[6,7,14]. Positive control HEK293 cells transfected with cDNA encoding neprilysin[15], but not those transfected with a mock vector, produced fluorescence signals that were completely inhibited by a specific inhibitor of neprilysin, thiorphan (**Fig. 1a**). We then examined the effect of nearly 50 reagents (**Supplementary Table 1** online) on neprilysin activity in primary neurons. Only the neuropeptide somatostatin reproducibly and significantly increased neuronal thiorphan-sensitive neprilysin activity (**Fig. 1b**). Somatostatin did not generate fluorescence signals in primary neurons prepared from neprilysin-deficient mice[7]. All of the other reagents tested either had little effect or only slightly reduced neprilysin activity. The effect of somatostatin on neprilysin activity was clearly concentration-dependent, with a half-maximal effective dose (ED_{50}) of 50 nM (**Fig. 1c**), slightly higher than the K_m values of somatostatin for somatostatin receptors, presumably owing to degradation of somatostatin during incubation. When we used primary neurons prepared from mice lacking somatostatin precursor (SSTP)[16], the percentage increase in neprilysin activity upon exposure to somatostatin was higher as compared to the response of neurons from $Sst^{+/+}$ mice (approximately 200% versus 160–180%). This suggests that endogenously generated somatostatin is also involved in regulating neprilysin activity in the present experimental paradigm. Similar to the physiological subcellular location of neprilysin in the brain, neprilysin activity appeared as puncta on neuronal processes rather than in or around soma (**Fig. 1d**).

We performed further mechanistic analyses of the somatostatin-induced increase in neprilysin activity in primary neurons. The effect of somatostatin peaked at around 24 h and lasted up to approximately 36 h (**Fig. 2a**). The

[1]Laboratory for Proteolytic Neuroscience, RIKEN Brain Science Institute, 2-1 Hirosawa, Wako-shi, Saitama 351-0198, Japan. [2]These authors contributed equally to this work. Correspondence should be addressed to T.C.S. (saido@brain.riken.go.jp) or N.I. (iwatan@brain.riken.go.jp).

Published online 20 March 2005; doi:10.1038/nm1206

decline after 24 h seems to be the result of somatostatin degradation and receptor desensitization because the quantity of exogenously administered somatostatin in culture media decreased to 19% in 36 h and readministration of somatostatin led to a smaller increase in neprilysin activity (<50% of the initial increase). We then inspected the effect of a somatostatin receptor antagonist[17] (BIM23056), a G_i inhibitor (pertussis toxin) and a G_s inhibitor (cholera toxin), on the somatostatin-induced elevation of neprilysin activity (**Fig. 2b**). BIM23056 and pertussis toxin, but not cholera toxin, inhibited neprilysin activation, indicating that G_i-coupled somatostatin receptors[18] are involved in the signal transduction leading to neprilysin activation. RT-PCR analysis using a set of primers that recognize all three neprilysin transcript variants[7] indicated that somatostatin administration did not change the quantity of mRNA 12 h after the treatment to an extent that can be detected by this method (data not shown). We also made efforts to detect neprilysin in primary neurons by immunocytochemistry and western blotting, but the protein levels were below the detection limit. The results indicate that the effect of somatostatin on the transcription of the gene encoding neprilysin, *Mme*, is limited and that somatostatin might have exerted its effect mainly through post-translational events. Notably, somatostatin treatment resulted in selective and significant reduction of $A\beta_{42}$, but not $A\beta_{40}$, in the culture media of primary neurons (**Fig. 2c**). Somatostatin did not induce this selective reduction of $A\beta_{42}$ when primary neurons prepared from neprilysin-knockout mice were used, indicating that neprilysin is directly involved in the somatostatin-regulated $A\beta_{42}$ metabolism (**Fig. 2d**).

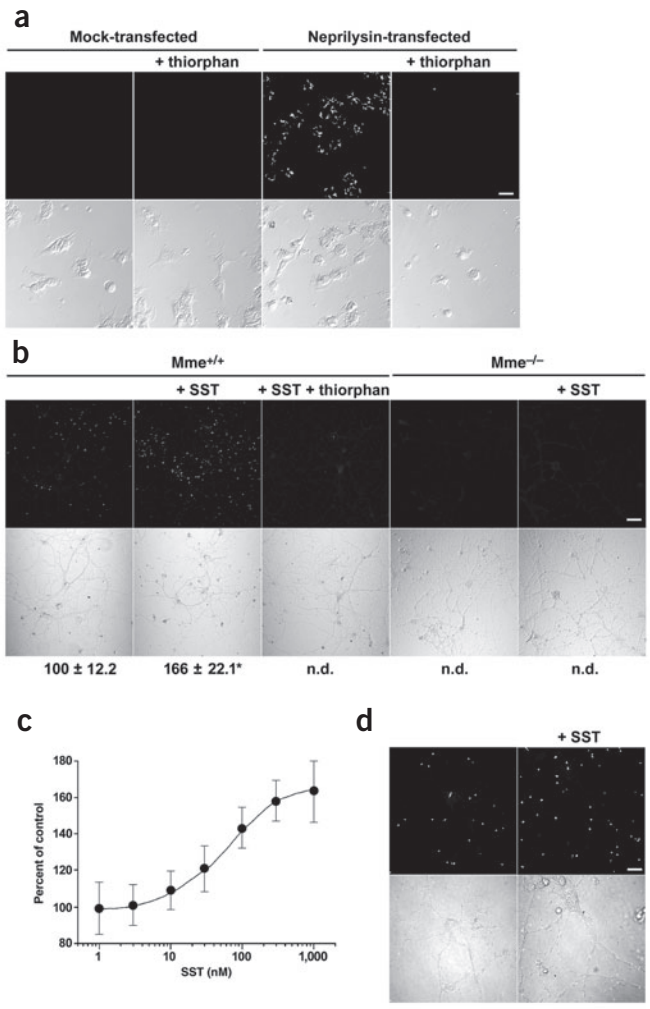

Because the above observations might be *in vitro* artifacts, we next investigated whether somatostatin contributes to the regulation of neprilysin activity and, consequently, of Aβ levels *in vivo* using SSTP knockout mice. These mice were developmentally and morphologically normal[16]. Immunofluorescence indicated that the level of hippocampal somatostatin, which is absent in the $Sst^{-/-}$ mouse brain, did not significantly differ between $Sst^{+/+}$ and $Sst^{+/-}$ mice (**Fig. 3a**), suggesting that the relationship between the somatostatin level and SSTP gene dosage is not linear. This presumably reflects the fact that transcription, mRNA stability, translation or post-translational processing of SSTP have a rate-limiting role in the generation of somatostatin to some extent. Neprilysin activity in the hippocampus of $Sst^{-/-}$ mice was significantly lower than in $Sst^{+/+}$ mice in agreement with the above *in vitro* observations, whereas the difference between $Sst^{+/+}$ mice and $Sst^{+/-}$ mice was not significant (**Fig. 3b**). Nevertheless, there was a tendency for the enzyme activity in $Sst^{+/-}$ mice to be consistently weaker.

We then quantified $A\beta_{40}$ and $A\beta_{42}$ levels in the hippocampus from $Sst^{+/+}$, $Sst^{+/-}$ and $Sst^{-/-}$ mice. Although somatostatin deficiency seemed to result in the elevation of both Aβ species, the increase in $A\beta_{42}$ in $Sst^{-/-}$ mice was statistically significant ($P = 0.0011$), but the increase in $A\beta_{40}$ was not ($P = 0.2221$). Thus, the effect of somatostatin deficiency was more pronounced for $A\beta_{42}$ in this brain region. The difference in the $A\beta_{42}/A\beta_{40}$ ratio was not statistically significant. (Therefore, the effect of somatostatin deficiency is similar, but not identical, to that of familial Alzheimer disease–causing mutations in presenilin genes, which selectively increase the level of $A\beta_{42}$ relative to $A\beta_{40}$.) This observation is consistent with the *in vitro* effect of somatostatin on the Aβ levels in culture media (**Fig. 2c**,**d**). The presence of cortistatin, a somatostatin homolog capable of activating somatostatin receptors, in the brain[19] might have contributed to the basal neprilysin activity in $Sst^{-/-}$ mice, although the nature of this relatively new neuropeptide family member has not yet been thoroughly explored.

In contrast, we observed no difference in neprilysin activity in the cerebellum between $Sst^{+/+}$ and $Sst^{-/-}$ mice (**Fig. 3c**). There was also no difference in the quantities of $A\beta_{40}$ or $A\beta_{42}$ in the cerebellum between $Sst^{+/+}$ and $Sst^{-/-}$ mice. These observations are in accordance with the human pathology of Aβ amyloidosis initially taking place in the hippocampus and the temporal cortex and only modestly affecting the cerebellum[9]. We also examined whether somatostatin deficiency affected APP metabolism in the hippocampus by western blot analysis of full-length APP, soluble extracellular APP fragment generated by α-secretase (APPsα), soluble extracellular APP fragment generated by β-secretase (APPsβ), C-terminal fragment (CTF)-β, CTF-α and CTF-γ (**Fig. 3d**,**e**). There was no difference in the quantity of APP or any of the APP fragments, whereas neprilysin expression was significantly reduced in $Sst^{-/-}$ mice, excluding the possibility that somatostatin might have affected Aβ levels through alteration of APP metabolism.

Figure 1 *In vitro* screening for a neprilysin activating ligand using primary neurons. (**a**) HEK293 cells transfected with mock vector or *Mme* cDNA[15] were subjected to activity staining in the presence and absence of 1 μM thiorphan as indicated. The upper panels are fluorescence images representing neprilysin activity and the lower panels are phase-contrast images. Bar, 20 μm. (**b**) Primary cortical neurons prepared from $Mme^{+/+}$ and $Mme^{-/-}$ mice treated with or without 1 μM somatostatin (SST; 14-mer) were analyzed by activity staining in the presence or absence of thiorphan as indicated. The fluorescence signals in the upper panels are superimposed on the phase-contrast images in the lower panels. Relative intensities of the fluorescence signals are indicated below each panel as an average ± s.d. ($n = 4$). n.d., not detectable. $^*P < 0.05$ as compared to controls. Bar, 120 μm. (**c**) Effect of somatostatin concentration on neprilysin activity. The bars indicate 1 s.d. ($n = 4$). (**d**) Higher power images of activity-stained primary neurons treated with somatostatin as above. Bar, 40 μm.

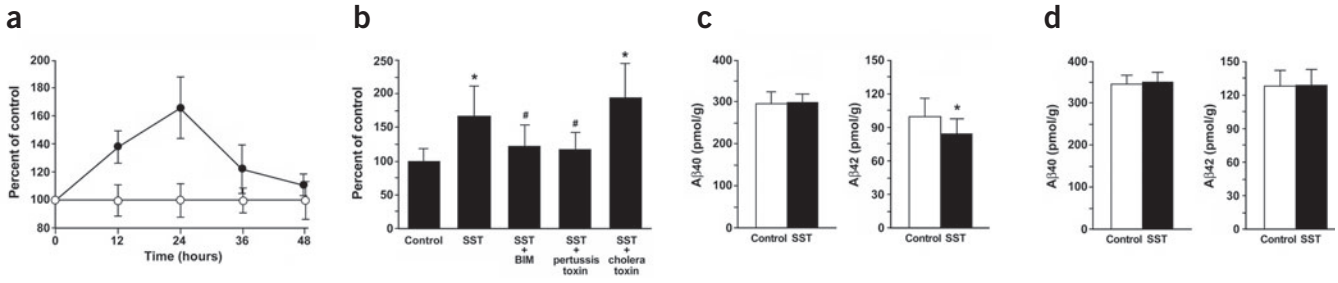

Figure 2 Mechanism of somatostatin action and effect on Aβ clearance *in vitro*. (**a**) Time course of neprilysin activity changes in primary neurons treated with (closed circles) or without (open circles) somatostatin as in **Figure 1b**. The bars indicate 1 s.d. ($n = 6$). (**b**) Effect of somatostatin receptor agonist BIM23056 (BIM, 100 μM), pertussis toxin (100 ng/ml) and cholera toxin (100 ng/ml) on the somatostatin (SST;1μm)-induced neprilysin activity. The bars indicate averages ± 1 s.d. ($n = 8$). *, $P < 0.05$ as compared to controls; #, $P < 0.05$ as compared to somatostatin-treated neurons by Student-Newman-Keuls multiple range test. (**c**) Effect of somatostatin treatment on the concentrations of $A\beta_{40}$ and $A\beta_{42}$ in the culture media of primary neurons prepared from wild-type mice. Culture media were collected 24 h after somatostatin treatment, and soluble Aβ levels were quantified as previously described[14]. The experiments were performed 7 d after neurons had been cultured at a concentration of 6×10^5 per well in 12-well plates. The bars indicate the averages ± 1 s.d. ($n = 12$). *, $P < 0.05$. (**d**) Effect of somatostatin treatment on the concentrations of $A\beta_{40}$ and $A\beta_{42}$ in the culture media of primary neurons prepared from neprilysin knockout mice. The experiments were performed in an identical manner for those in **c** ($n = 12$).

Somatostatin deficiency reduced *Mme* transcription only slightly (by 15% as analyzed by northern blotting, although this decrease was statistically significant; **Fig. 3e**), so the effect of somatostatin on neprilysin is probably mediated mostly by post-translational processes such as metabolism and cellular localization of neprilysin, as implied by the *in vitro* experiments. The difference in the activity and quantity of neprilysin between $Sst^{+/+}$ and $Sst^{-/-}$ mice was already demonstrated (**Fig. 3b**,**d**,**e**), but we also investigated a possible alteration of neprilysin localization in hippocampus by a triple immunofluorescence technique using antibodies against neprilysin (red), vesicular GABA transporter (VGAT; green) and tau (blue) (**Fig. 4a**). Quantification of the results by image analysis indicated that somatostatin deficiency significantly reduced neprilysin expression in the outer molecular layer of dentate gyrus to 78% (**Fig. 4b**). Colocalization of neprilysin with a presynapse marker, VGAT, was reduced even further in both lacunosum moleculare and outer molceluar layer, to 58% and to 68%, respectively (**Fig. 4c**), whereas colocalization with an axonal marker, tau, remained unchanged (**Fig. 4d**). These observations, indicating that somatostatin also regulates presynaptic localization of neprilysin, were confirmed by biochemical fractionation of cortical tissues showing that synaptic membrane-associated neprilysin was reduced and that ER-Golgi-microsome-associated neprilysin was increased in $Sst^{-/-}$ mice while synaptic vesicle-associated neprilysin remained unchanged (**Supplementary Fig. 1** online).

The relatively high expression of somatostatin-induced neprilysin activity on the cell surface both *in vitro* (**Fig. 1**) and *in vivo* (**Fig. 4**) might perhaps account for the more pronounced effect of somatostatin on $A\beta_{42}$ levels (**Fig. 2c** and **Fig. 3c**). Whereas neprilysin deficiency resulted in increases of both $A\beta_{40}$ and $A\beta_{42}$ in an identical manner[7], infusion of the brain with the cell-impermeable neprilysin inhibitor, thiorphan, elevated $A\beta_{42}$ but not $A\beta_{40}$[6]. This suggests that $A\beta_{40}$ is largely degraded intracellularly, whereas $A\beta_{42}$ degradation takes place on or near the cell surface *in vivo*. We recently confirmed such differential cellular degradation of $A\beta_{40}$ and $A\beta_{42}$ by expressing chimeric neprilysin constructs targeted to different cellular compartments in primary cortical neurons[14]. The 'cell surface' probably corresponds to the outer surface of presynaptic processes *in vivo*. A possible explanation for the differential intra- and extracellular degradation of $A\beta_{40}$ and $A\beta_{42}$ may be the acidic conditions inside secretory vesicles, in which the pH is around 5 (ref. 20). We examined degradation of synthetic $A\beta_{40}$ and $A\beta_{42}$ by recombinant human neprilysin at pH 5.0 and pH 7.2 and found that, whereas $A\beta_{40}$ was degraded to the same extent under these different pH conditions, $A\beta_{42}$ degradation was reduced to approximately one-tenth at pH 5.0 as compared to that at pH 7.2 (**Supplementary Fig. 2** online). Although this result is consistent with the notion that $A\beta_{42}$ degradation occurs largely on or near the cell surface rather than inside secretory vesicles, there remains a possibility that another somatostatin-induced Aβ-degrading mechanism may exist in neurons. The mechanism of the somatostatin-induced neprilysin translocation remains unclear but might be associated with soluble *N*-ethylmaleimide–sensitive factor attachment protein receptor (SNARE) proteins involved in intracellular membrane fusion because the quantity of syntaxin, a SNARE family member, in the synaptic vesicle fraction was apparently increased in $Sst^{-/-}$ mice (**Supplementary Fig. 1** online). There also remains a possibility that unknown neprilysin-interacting or modifying factors might be involved.

The finding that the amount of $A\beta_{42}$ increased around 1.5-fold in the brain of somatostatin-deficient mice is interesting given that an elevation of $A\beta_{42}$ is the common phenotype of virtually all of the familial AD-causing gene mutations[5]. Notably, it has been shown that SSTP mRNA is one of the very few transcripts (0.5% of 11,000 examined) consistently reduced in human brains upon aging[2]. These observations lead us to draw the following hypothetical scenario for development of late-onset sporadic Alzheimer disease. Downregulation of somatostatin and, possibly, related neuropeptide(s)[19] in human brain in the early stage of aging may initiate gradual elevation of Aβ levels by lowering neprilysin activity and, in a decade or two, lead to Aβ amyloidosis that eventually triggers a cascade of Alzheimer disease–associated pathological events.

Our findings also indicate that increasing somatostatin concentration or agonizing somatostatin receptors in the brain will contribute to the clearance of this primary pathogenic form of Aβ when somatostatin levels in the brain drop to as low as 10–20% of control levels during aging or Alzheimer disease development[1,3]. Also notable is the fact that somatostatin is likely to be directly involved in memory formation apart from its involvement in Aβ regulation[19]. This suggests that agonizing somatostatin receptors in brain may generate dual independent benefits for the improvement of neuronal function. Thus far, there have been five somatostatin receptor subtypes identified, all of which are G-protein-coupled receptors[19]. Among the five receptor subtypes, types two and four may be the primary candidate targets because they are relatively potently expressed in neocortex and hippocampus[19,21].

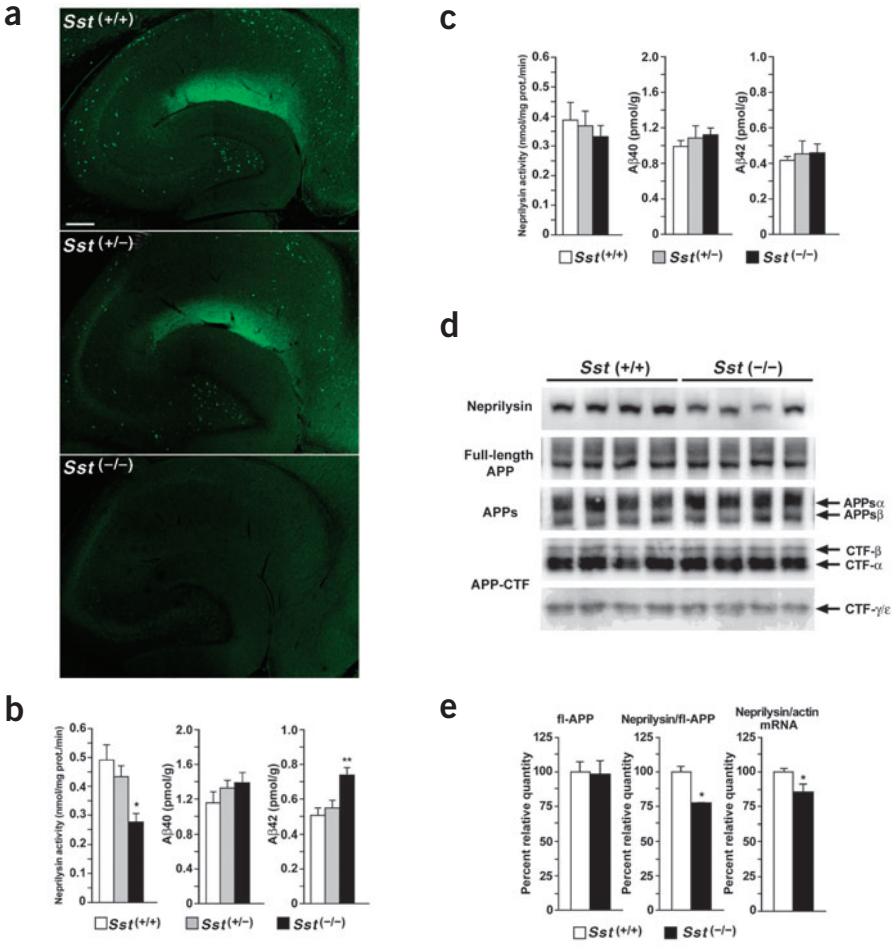

Figure 3 Neprilysin activities, Aβ levels and APP metabolism in somatostatin-deficient mouse brains. (**a**) Hippocampal sections from *Sst*$^{+/+}$, *Sst*$^{+/-}$ and *Sst*$^{-/-}$ mice (10–12 weeks old) as indicated were immunostained with anti-somatostatin antibody. Bar, 200 μm. (**b**) Hippocampal neprilysin activities and Aβ levels in *Sst*$^{+/+}$, *Sst*$^{+/-}$ and *Sst*$^{-/-}$ mice. The bars indicate averages ± s.e.m. ($n = 14$ for *Sst*$^{+/+}$, $n = 21$ for *Sst*$^{+/-}$ and 10 for *Sst*$^{-/-}$). (**c**) Cerebellar neprilysin activities and Aβ levels in *Sst*$^{+/+}$, *Sst*$^{+/-}$ and *Sst*$^{-/-}$ mice. (**d**) Western blot analysis of neprilysin, full-length APP (fl-APP), APPsα, APPsβ, CTF-β, CTF-α and CTF-γ in the hippocampus of *Sst*$^{+/+}$ and *Sst*$^{-/-}$ mice. A monoclonal antibody, 22C11, was used to detect fl-APP and APPs; a polyclonal antibody, A8717, against the C-terminal region of APP was used to detect CTF-β, CTF-α and CTF-γ. (**e**) Quantification of fl-APP immunoreactivity, neprilysin immunoreactivity normalized against fl-APP ($n = 8$) and neprilysin mRNA normalized against actin mRNA ($n = 4$) in the hippocampus of *Sst*$^{+/+}$ and *Sst*$^{-/-}$ mice. *Mme* and *Actb* mRNA levels were quantified by northern blotting. Reduction of *Mme* mRNA in *Sst*$^{-/-}$ mice was also confirmed by quantitative RT-PCR for type 1 transcript. * $P < 0.05$; ** $P < 0.002$.

Synthesis of blood brain barrier–permeable agonists that can distinguish between different somatostatin receptor subtypes, or such use of an 'antidementia' compound as FK960 that elevates hippocampal somatostatin levels[22] in the brain may be potential approaches to reducing Aβ levels. One potential benefit of harnessing neprilysin activity by agonizing somatostatin receptors, among other Aβ-reducing strategies, is that, if used modestly, it is unlikely to accompany major adverse side effects because a deficiency of neprilysin does not seem to alter the levels of 'neprilysin substrate' neuropeptides such as enkephalin, cholecystokinin, neuropeptide Y, substance P and somatostatin in the brain (N.I. & T.C.S., unpublished data), indicating the presence of redundant buffering mechanisms to metabolize these peptides. This new approach might be combined with other approaches targeting at β-secretase[23] and γ-secretase[24] as a cocktail therapy strategy to achieve a selective effect on Aβ levels in the brain with minimum adverse side effects.

METHODS

Activity staining of primary neurons. Cortical neurons were isolated from embryonic C57BL/6J mice at the development stage of 16–18 d as previously described[25]. Cells (1×10^5 cells) were cultured on poly-L-lysine (PLL)-coated glass cover slips (12 mm/0.12–0.17 mm thickness; Matsunami) in 24-well plate (Iwaki). AraC (final concentration, 1 μM) was added after the first 3 d of culture, and the culture medium was changed once per week thereafter and 4 h before treatment. After 28 d *in vitro*, cultured neurons were treated with one of the reagents listed in **Supplementary Table 1** online for 24 h at 37 °C, and this process repeated on different cultures for each of the reagents. Cells were then washed twice with Tris-buffered saline (pH 7.4), fixed with 1.5% paraformaldehyde in 50 mM phosphate buffer (pH 6.8) for 12 min at 20 °C, and washed twice with the Tris-buffered saline for subsequent staining for neprilysin activity. The fixed neurons were incubated in 0.2 ml of substrate solution (0.5 mM glutaryl-Ala-Ala-Phe-methoxy-2-naphthylamide[26] (Sigma) in 62.5 mM Tris-HCl (pH 7.4)) at 4 °C for 48 h. Leucine aminopeptidase, phosphoramidon and nitrosalicylaldehyde were then added to the substrate solution at final concentrations of 50 μg/ml, 10 μM and 0.6 mM, respectively, and incubated for 0.5 h at 37 °C. The cells were rinsed twice with ice-cold 50 mM Tris-HCl (pH 7.4) and subjected to immunofluorescence analysis with a filter for rhodamine visualization using argon laser excitation. The activity staining is used to visualize neprilysin activity on the cell surface because leucine-aminopeptidase does not enter the cells. We also made efforts to perform intracellular activity staining by permeabilizing cells with detergents but did not succeed because detergent treatment resulted in destruction of cell structures in the present experimental paradigm. Quantification of fluorescence images was performed as previously described[8,11]. All animal experiments were performed in compliance with the institutional guidelines.

RT-PCR and northern blot analysis. RT-PCR to detect *Mme* mRNA was carried out using total RNA as previously described[27] with the following pairs of primers: 5′-GCTGTAGTCAATGCATT-3′ and 5′-GAAAGGCATCTGCAAAC-3′ for all three types of transcripts; 5′-CTCAGTCGCCTCCAACTTCTCC-3′ and 5′-GCATAGAGAGCGATCATTGTCACC-3′ for type 1 transcript[7]. The following pair of primers for gyceraldehyde-3-phospate dehydrogenase was used for calibration: 5′-TGACCACAGTCCATGCCATCAC-3′ and 5′-TCCACCACCCTGTTGCTG-3′. PCR products were electrophoresed on 5% polyacrylamide gels. Gels were stained with ethidium bromide (1 μg/ml), and then DNA fragments were visualized by UV illumination and photographed. For northern blotting, polyadenylated RNA was isolated from hippocampus using Micro-Fast Track 2.0 kit (Invitrogen). Samples were electrophoresed in 1% formaldehyde agarose gels and transferred to nylon membranes. The membranes were probed with a [α-^{32}P]dCTP-labeled 520-base-pair mouse *Mme* cDNA fragment generated by PCR using a pair of primers, 5′-GCTGTAGTCAATGCATT-3′ and 5′-GAAAGGCATCTGCAAAC-3′. The gels were stained with ethidium bromide and the membranes were reprobed with an actin cDNA (Sigma) to confirm the quantity of loaded DNAs.

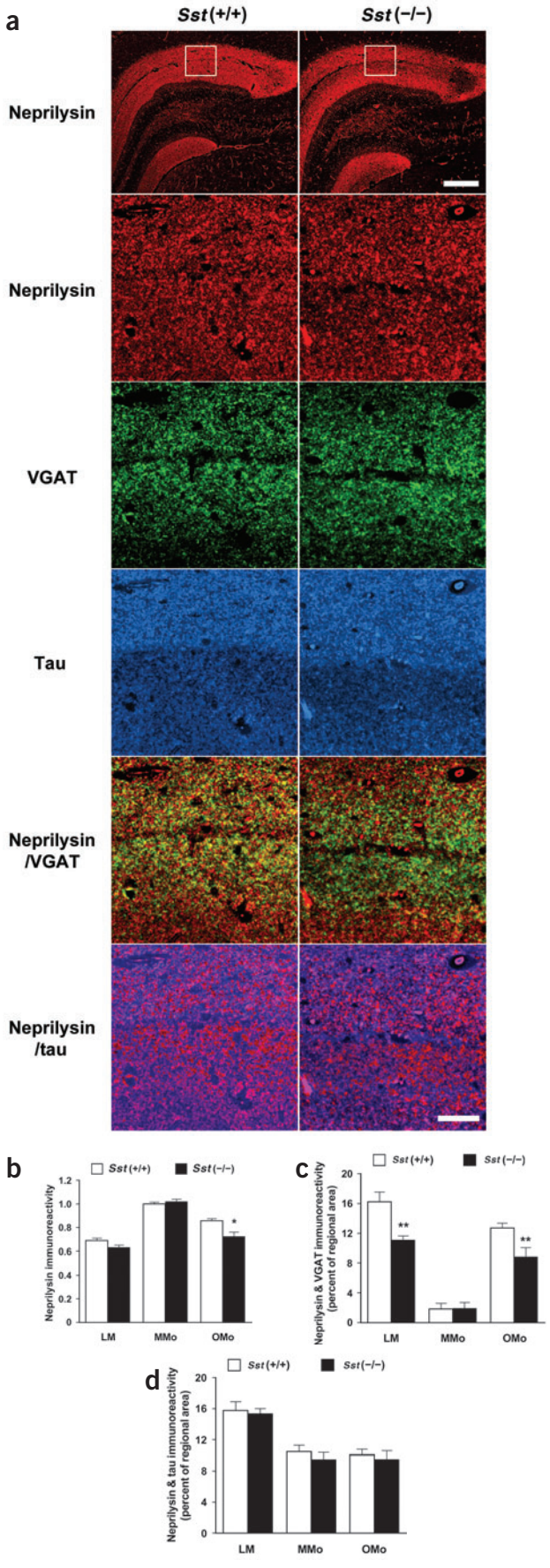

Figure 4 Localization of neprilysin immunoreactivity in $Sst^{+/+}$ and $Sst^{+/-}$ mice. (**a**) Hippocampal sections from $Sst^{+/+}$ mice (left panels) and $Sst^{-/-}$ mice (right panels) were subjected to triple-immunofluorescence examination using antibodies to neprilysin (red), VGAT (green), and tau (blue) as indicated. Superimposed images of neprilysin-VGAT and neprilysin-tau are shown in the lower two pairs of panels. Areas indicated by squares in the top panels were quantitatively analyzed at higher resolution. Bars, 200 μm in the top panels and 40 μm in the others. (**b**) Neprilysin immunoreactivity in stratum lacunosum-moleculare (LM), middle molecular layer (MMo) and outer molecular layer (OMo) was quantified by image analysis. The bars represent averages ± s.e.m. ($n = 4$). (**c**) Colocalization of neprilysin and VGAT, as an indicator of presynapse-associated neprilysin, was quantified as in **b**. (**d**) Colocalization of neprilysin and tau, as an indicator of axon-associated neprilysin, was quantified as in **b**. $^{*}P < 0.05$; $^{**}P < 0.01$.

Immunochemical procedures. Somatostatin immunostaining of brain sections was performed as described[28] using a rabbit anti-somatostatin antiserum, T-4103 (Peninsula). The assay for brain tissue neprilysin was described previously in detail[8,11]. Quantification of brain $A\beta_{40}$ and $A\beta_{42}$ was performed using sandwich ELISA with antibodies BNT77/BA27 and BNT77/BC05 as previously described[7,11]. Western blot analyses of APP and APP fragments were performed using a monoclonal antibody to the N-terminal region of APP (22C11; Chemicon) and a rabbit polyclonal antibody to the C-terminal region of APP (A8717; Sigma). Western blot analysis of neprilysin was performed as described[11,14] except that a polyclonal antibody (421126; Techne) was used. Immunoreactive signals were detected with ECL Advance Western Blotting Detection kit (Amersham) and quantified with a LuminoImager, LAS-3000 and Science Lab 2001 Image Gauge software (Fuji Photo Film). For triple-immunofluorescence analysis of the hippocampal formation, representative 4-μm thick paraffin sections were stained with antibodies against neprilysin (mouse monoclonal 56C6, 1:400; Novocastra), VGAT (rabbit polyclonal 117G4, 1:1,500; Synaptic Systems) and tau (T49, mouse monoclonal, 1:500; gift of J. Trojanowski and V. M.-Y. Lee, University of Pennsylvania School of Medicine) based on the previously described method[29] with a TSA-Direct kit (NEN Life Science Products). Specificity of neprilysin staining was confirmed using neprilysin-deficient mice as a negative control[8]. Quantification of immunofluorescence images was performed using MetaMorph (version 6.1) imaging software (Universal Imaging Corporation) as previously described[8,11]. The statistical significance was examined by Student's *t*-test after confirming the equality between the group variances unless otherwise stated.

Other reagents. BIM23056 was synthesized in the Research Resource Center, RIKEN BSI. Pertussis toxin and cholera toxin were purchased from CalBiochem and Sigma, respectively.

Note: Supplementary information is available on the Nature Medicine website.

ACKNOWLEDGMENTS

We thank E. Hosoki, M. Sekiguchi, Y. Matsuba, N. Yamazaki and K. Watanabe for technical assistance and A. Miyawaki for valuable discussions. We express our gratitude to U. Hochgeschwender, Oklahoma Medical Research Foundation for providing SSTP knockout mice and helpful comments. We also thank Takeda Chemical Industries Ltd. and C. Gerard, Harvard Medical School, for providing the monoclonal antibodies to Aβ for ELISA and neprilysin knockout mice, respectively. The research was supported by research grants from RIKEN Brain Science Institute, the Ministry of Education, Culture, Sports, Science and Technology of Japan, and Life Science Foundation (Tokyo).

COMPETING INTERESTS STATEMENT

The authors declare that they have no competing financial interests.

Received 25 August 2004; accepted 3 January 2005
Published online at http://www.nature.com/naturemedicine/

1. Hayashi, M., Yamashita, A. & Shimizu, K. Somatostatin and brain-derived neurotrophic factor mRNA expression in the primate brain: decreased levels of mRNA during aging. *Brain Res.* **749**, 283–289 (1997).
2. Lu, T. *et al.* Gene regulation and DNA damage in the ageing human brain. *Nature* **429**, 883–891 (2004).
3. Davies, P., Katzman, R. & Terry, R.D. Reduced somatostatin-like immunoreactivity in

cerebral cortex from cases of Alzheimer's disease and Alzheimer senile dementia. *Nature* **288**, 279–280 (1980).
4. van de Nes, J.A.P., Sandmann-Keil, D. & Braak, H. Interstitial cells subjacent to the entorhinal region expressing somatostatin-28 immunoreactivity are susceptible to development of Alzheimer's disease–related cytoskeletal changes. *Acta Neuropathol.* **104**, 351–356 (2002).
5. Hardy, J. & Selkoe, D.J. The amyloid hypothesis of Alzheimer's disease: progress and problems on the road to therapeutics. *Science* **297**, 353–356 (2002).
6. Iwata, N. *et al.* (2000). Identification of the major $A\beta_{1-42}$-degrading catabolic pathway in brain parenchyma: Suppression leads to biochemical and pathological deposition. *Nat. Med.* **6**, 143–151 (2000).
7. Iwata, N. *et al.* Metabolic regulation of brain Aβ by neprilysin. *Science* **292**, 1550–1552 (2001).
8. Iwata, N., Takaki, Y., Fukami, S., Tsubuki, S. & Saido, T.C. Region-specific reduction of Aβ-degrading endopeptidase, neprilysin, in mouse hippocampus upon aging. *J. Neurosci. Res.* **70**, 493–500 (2002).
9. Yasojima, K., Akiyama, H., McGeer, E.G. & McGeer, P.L. Reduced neprilysin in high plaque areas of Alzheimer brain: a possible relationship to deficient degradation of β-amyloid peptide. *Neurosci. Lett.* **297**, 97–100 (2001).
10. Leissring, M.A. *et al.* Enhanced proteolysis of β-amyloid in APP transgenic mice prevents plaque formation, secondary pathology, and premature death. *Neuron* **40**, 1087–1093 (2003).
11. Iwata, N. *et al.* Presynaptic localization of neprilysin contributes to efficient clearance of amyloid-β peptide in mouse brain. *J. Neurosci.* **24**, 991–998 (2004).
12. Wang, T.-L., Chang, H., Hung, C.-R. & Tseng, Y.-Z. Morphine preconditioning attenuates neutrophil activation in rat models of myocardial infarction. *Cardiovasc. Res.* **40**, 557–563 (1998).
13. Joshi, D.D. *et al.* Negative feedback on the effect of stem cell factor on hematopoiesis is partly mediated through neutral endopeptidase activity on substance P: a combined functional and proteomic study. *Blood* **98**, 2697–2706 (2001).
14. Hama, E., Shirotani, K., Iwata, N. & Saido, T.C. Effects of neprilysin chimeric proteins targeted to subcellular compartments on amyloid β peptide clearance in primary neurons. *J. Biol. Chem.* **279**, 30259–30269 (2004).
15. Shirotani, K. *et al.* Neprilysin degrades both amyloid β peptides 1–40 and 1–42 most rapidly and efficiently among thiorphan- and phosphoramidon-sensitive endopeptidases. *J. Biol. Chem.* **276**, 21895–21901 (2001).
16. Zeyda, T., Diehl, N., Paylor, R., Brennan, M.B. & Hochgeschwender, U. Impairment in motor learning of somatostatin null mutant mice. *Brain Res.* **906**, 107–114 (2001).
17. Shimon, I. *et al.* Somatostatin receptor subtype specificity in human fetal pituitary cultures. *J. Clin. Invest.* **99**, 789–798 (1997).
18. Garcia-Jimenez, A., Fastbom, J., Winbland, B. & Cowburn, R.F. G-protein regulation of signal transduction in Alzheimer's disease. *Brain Aging* **2**, 7–15 (2002).
19. Moller, L.N., Stidsen, C.E., Hartmann, B. & Holst, J.J. Somatostatin receptors. *Biochim. Biophys. Acta* **1616**, 1–84 (2003).
20. Miesenbock, G., De Angelis, D.A. & Rothman, J.E. Visualizing secretion and synaptic transmission with pH-sensitive green fluorescent proteins. *Nature* **394**, 192–195 (1998).
21. Bruno, J.F., Xu, Y., Song, J. & Berelowitz, M. Molecular cloning and functional expression of a brain-specific somatostatin receptor. *Proc. Natl. Acad. Sci. USA* **89**, 11151–11155 (1992).
22. Doggrell, S.A. The potential of activation of somatostatinergic neurotransmission with FK960 in Alzheimer's disease. *Expert Opin. Investig. Drugs* **13**, 69–72 (2004).
23. Citron, M. β-Secretase: progress and open questions. in *Aβ Metabolism and Alzheimer's Disease.* (ed. Saido, T.C.) 17–25 (Landes Bioscience, Georgetown, 2003).
24. Wolfe, M.S. γ-Secretase and presenilin. in *Aβ Metabolism and Alzheimer's Disease.* (ed. Saido, T.C.) 33–47 (Landes Bioscience, Georgetown, 2003).
25. Hama, E. *et al.* Clearance of extracellular and cell-associated amyloid β peptide by viral expression of neprilysin in primary culture. *J. Biochem.* **130**, 721–726 (2001).
26. Back, S.A. & Gorestein, C. Histochemical visualization of neutral endopeptidase-24.11 (enkephalinase) activity in rat brain: cellular localization and codistribution with enkephalins in the globus pallidus. *J. Neurosci.* **9**, 4439–4455 (1989).
27. Takano, J., Watanabe, M., Hitomi, K. & Maki, M. Four types of calpastatin isoforms with distinct amino-terminal sequences are specified by alternative first exons and differentially expressed in mouse tissues. *J. Biochem.* **128**, 83–92 (2000).
28. Jinno, S. & Kosaka, T. Patterns of expression of neuropeptides in GABAergic nonprincipal neurons in the mouse hippocampus: Quantitative analysis with optical disector. *J. Comp. Neurol.* **461**, 333–349 (2003).
29. Wang, G. *et al.* Tyramide signal amplification method in multiple-label immunofluorescence confocal microscopy. *Methods* **18**, 459–464 (1999).